Cancellation of Coherent Synchrotron Radiation Kicks with Optics Balance

S. Di Mitri,[1] M. Cornacchia,[1] and S. Spampinati[2]

[1]*Elettra-Sincrotrone Trieste S.C.p.A., 34149 Basovizza, Trieste, Italy*

[2]*University of Nova Gorica, SI-5000 Nova Gorica, Slovenia*

(Received 6 August 2012; revised manuscript received 24 September 2012; published 2 January 2013)

Minimizing transverse emittance is essential in linear accelerators designed to deliver very high brightness electron beams. Emission of coherent synchrotron radiation (CSR), as a contributing factor to emittance degradation, is an important phenomenon to this respect. A manner in which to cancel this perturbation by imposing certain symmetric conditions on the electron transport system has been suggested.We first expand on this idea by quantitatively relating the beam Courant-Snyder parameters to the emittance growth and by providing a general scheme of CSR suppression with asymmetric optics, provided it is properly balanced along the line. We present the first experimental evidence of this cancellation with the resultant optics balance of multiple CSR kicks: the transverse emittance of a 500 pC, sub-picosecond, high brightness electron beam is being preserved after the passage through the achromatic transfer line of the FERMI@Elettra free electron laser, and emittance growth is observed when the optics balance is intentionally broken. We finally show the agreement between the theoretical model and the experimental results. This study holds the promise of compact dispersive lines with relatively large bending angles, thus reducing costs for future electron facilities.

DOI: 10.1103/PhysRevLett.110.014801 PACS numbers: 29.27.Bd, 29.20.Ej, 29.27.Eg, 41.60.Ap

The advent of sub-picosecond electron beams with very high brightness in x-ray free electron lasers (FELs) [1–7] and in linear colliders [8,9] has raised the awareness of the accelerator community to the effect of the coherent synchrotron radiation (CSR) on beam transverse emittance [10,11]. The works reported in Refs. [12–16] trace the theoretical understanding of the CSR effects for ultrarelativistic beams. Experiments supporting that understanding may be found in Refs. [17–19]. In summary, the CSR field affects the electron transverse motion both with radial forces and by changing the particle energy in the dispersive line. In the latter case, the particle starts a betatron oscillation around a new reference trajectory, thus increasing its Courant-Snyder (C-S) invariant [2]. The synchrotron radiation emission is coherent for wavelengths comparable to the electron bunch length, and it induces a variation of the particle energy that is correlated with the longitudinal coordinate along the bunch. The removal of this correlation suppresses the CSR-driven emittance growth [1,20].

We have observed the suppression of the CSR-driven emittance excitation in the double bend achromatic system of the FERMI@Elettra FEL [3], with good agreement between the model prediction and the experimental results. The idea originally reported in Ref. [1] is reviewed using the C-S formalism. This treatment permits us to explicitly relate the optics (a) symmetry and the emittance growth, and thus to envisage possible alternative designs of a dispersive line in the presence of constraints other than optical. Our analysis considers the effect of the CSR on the particle transverse motion through the momentum dispersion only, justified by the fact that the kick provided by the radial forces defined as F_x^{eff} and G_{res} in Ref. [16] is small ($\leq 10^{-6}$) compared to $\theta\delta \approx 10^{-5}$, the product of the bending angle and the CSR-induced relative energy deviation. The effect of radiation shielding [21–23] is neglected, since the wavelength at which the CSR starts being suppressed by the vacuum chamber [22], $\lambda \geq 2h(h/R)^{1/2} \cong$ 1 mm (h is the vacuum chamber gap and R the bending radius), is much longer than the electron bunch length, 40 μm $\leq \sigma_z \leq$ 80 μm. Particle-field interactions on a scale much shorter than the bunch length such as those driving the so-called microbunching instability [24–27] are ignored on the ground that the analysis of the microbunching instability [26,27] predicts a small gain for the experimental configuration of this study. For the sake of simplicity, the CSR emission and its interaction with the electrons is described below within the bounds of the single-kick approximation. The beam is ultrarelativistic and with a small energy spread relative to the mean energy (σ_δ), so that the small momentum compaction (R_{56}) of the FERMI achromatic system does not significantly change either the bunch length or the longitudinal charge distribution, at any point of the lattice ($|R_{56}\sigma_\delta| \leq 5$ μm $\ll \sigma_z$). This is an important condition since it implies the same CSR energy kick in all the dipoles, and it eventually allows the removal of the energy-position correlation established by the radiation emission. The relatively small σ_δ also allows us to neglect chromatic aberrations. The FERMI achromatic system, denoted henceforth as Spreader, is made of two identical double bend achromats (denoted henceforth as MDBA) [3,28], as sketched in Fig. 1. We recall that in a (M)DBA with identical dipoles $|\eta|$ and $|\frac{d\eta}{ds}|$ (s is the longitudinal coordinate along the beam line) are the same, respectively, in all the dipoles [2,29].

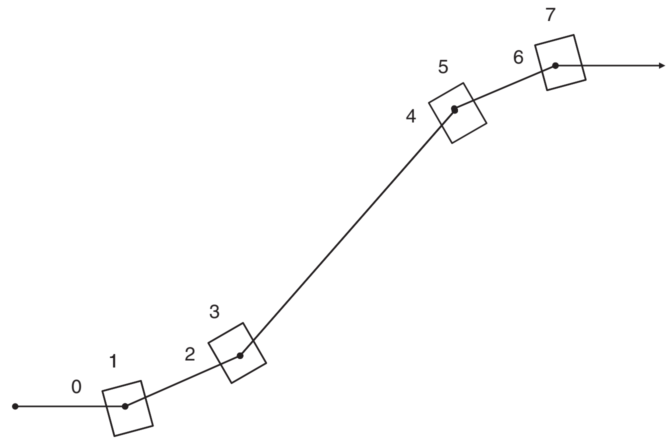

FIG. 1. The FERMI Spreader (not to scale). The design optics gives a betatron phase advance of π in the bending plane between two consecutive dipoles. There are quadrupoles between the dipoles (not shown here).

Each FERMI MDBA includes two focusing-defocusing cells, and their nominal setting ensures $\Delta\mu = \pi$ between the dipoles and a symmetric β and α, with values β_1 (α_1) and β_4 (α_4) in the dipoles of the first and the second achromat, respectively (see Table I). The two MDBAs are separated by seven quadrupoles with a phase advance of π between them. In the following, the C-S formalism is applied to the particle motion in the Spreader with the aforementioned notation. Only the motion in the bending plane is considered.

The initial particle coordinates relative to the reference trajectory are $x_0 = 0$, $x'_0 = 0$, and the initial particle invariant is $2J_0 = 0$. The variable subscript refers to the point along the lattice, as indicated in Fig. 1. After the CSR kick in the first dipole, the particle transverse coordinates become [2]

$$\begin{aligned} x_1 &= \eta\delta \equiv \sqrt{2J_1\beta_1}\cos\Delta\mu|_{\Delta\mu=0} = \sqrt{2J_1\beta_1}, \\ x'_1 &= \eta'\delta \equiv -\sqrt{\frac{2J_1}{\beta_1}}(\alpha_1\cos\Delta\mu + \sin\Delta\mu)|_{\Delta\mu=0} \\ &= -\alpha_1\sqrt{\frac{2J_1}{\beta_1}}. \end{aligned} \tag{1}$$

After the CSR kick, the particle C-S invariant has grown to $2J_1 = \gamma_1 x_1^2 + 2\alpha_1 x_1 x'_1 + \beta_1 x_1'^2 = H_1\delta^2$, where $H_1 = \gamma_1\eta^2 + 2\alpha_1\eta\eta' + \beta_1\eta'^2$ and $\gamma_1 = (\frac{1+\alpha_1^2}{\beta_1})$. At the second dipole, after π phase advance and in the presence of the second CSR kick we have

$$\begin{aligned} x_3 &= x_2 + \eta\delta = -\sqrt{2J_1\beta_2} + \sqrt{2J_1\beta_1} = 0, \\ x'_3 &= x'_2 - \eta'\delta = \alpha_2\sqrt{\frac{2J_1}{\beta_2}} + \alpha_1\sqrt{\frac{2J_1}{\beta_1}} = \sqrt{\frac{2J_1}{\beta_1}}(\alpha_1 + \alpha_2). \end{aligned} \tag{2}$$

Equation (2) was obtained by substituting the dispersive terms as in Eq. (1) and by using the symmetry of β at the dipoles (no specific choice for α is made at this stage). The same steps followed so far can easily be repeated till the end of the line. A new invariant will be defined after each CSR kick by the algebraic addition of the dispersive terms to the particle coordinates. With the additional equality $2J_i = \gamma_i x_i^2 + 2\alpha_i x_i x'_i + \beta_i x_i'^2$ for $i = 3, 5, 7$, each invariant J_i will be expressed as a function of J_1 and the C-S parameters. Doing this, after the last CSR kick we obtain

$$\begin{aligned} x_7 &= \sqrt{2X_{15}J_1\beta_4} - \sqrt{2J_1\beta_1}, \\ x'_7 &= -\alpha_7\sqrt{\frac{2X_{15}J_1}{\beta_4}} - \alpha_1\sqrt{\frac{2J_1}{\beta_1}}, \end{aligned} \tag{3}$$

TABLE I. Parameters of the electron beam (measured) and of the Spreader (by design). The optical functions are at the end of the dipole magnets. The beam parameters refer to compression factors of 8 and 16.

Parameter	Value	Units
Charge	500	pC
Mean energy	1240/1155	MeV
Energy spread, rms	0.24/0.06	%
Compression factor	8/16	
Final bunch length, rms	80/40	μm
Initial norm. emittance, rms	$2.3 \pm 0.1/1.9 \pm 0.1$	μm rad
Dipole bending angle	52	mrad
Dipole length	366	mm
Momentum dispersion (abs. value)	9	mm
Derivative of dispersion (abs. value)	50	mrad
Betatron function (1st and 2nd MDBA)	5.8, 2.9	m
Alpha function (1st and 2nd MDBA)	0.05, −0.30	
H_1 function	15	mm
$\|R_{56}\|$	2.1	mm

in which we defined

$$X_{15} = \frac{J_5}{J_1} = \frac{\beta_1}{\beta_4} + \left(\alpha_1\sqrt{\frac{\beta_4}{\beta_1}} - \alpha_5\sqrt{\frac{\beta_1}{\beta_4}}\right)^2 + \alpha_5(\alpha_1 + \alpha_3) \times \left[\alpha_5(\alpha_1 + \alpha_3) - 2\alpha_1\sqrt{\frac{\beta_4}{\beta_1}} + 2\alpha_5\sqrt{\frac{\beta_1}{\beta_4}}\right]. \quad (4)$$

The particle invariant at the end of the line is

$$2J_7 = 2J_1\left[\left(\sqrt{X_{15}} - \sqrt{\frac{\beta_1}{\beta_4}}\right)^2 + \left(\alpha_1\sqrt{\frac{\beta_4}{\beta_1}} + \alpha_7\sqrt{\frac{\beta_1}{\beta_4}}\right)^2\right] \equiv 2J_1X_{17}. \quad (5)$$

Equations (2)–(5) assume a constant value of β and α through the dipole magnet. By replacing the nominal values of β and α at the FERMI dipoles'entrance and exit into Eq. (5), one obtains, respectively, $X_{17} = 0.12$ and $X_{17} = 0.16$ that is a cancellation of the CSR effect for any practical purpose. A careful analysis of Eqs. (4) and (5) for the simpler case $\beta_1 = \beta_4$ shows that $J_7 = 0$ if $\alpha_1 = -\alpha_3 = \alpha_5 = -\alpha_7$. In summary, the simplest lattice for the cancellation of the CSR kicks is made of two identical, symmetric DBAs. Each achromat guarantees the proper phase advance and the symmetry of the C-S parameters required by Eq. (5). The additional constraint that one has to satisfy is the $(2n + 1)\pi$ phase advance between the two achromats, with n an integer. If a lattice design satisfies the latter condition but *not* the optics symmetry, the normalized rms emittance growth owing to the lack of complete CSR suppression will be given by the square-root sum of the unperturbed emittance and Eq. (5) averaged over the beam particle ensemble:

$$\Delta\gamma\varepsilon = \gamma\varepsilon\left[\sqrt{1 + \frac{H_1\sigma^2_{\delta,\mathrm{CSR}}}{\varepsilon}X_{17}} - 1\right], \quad (6)$$

where we used $2J_1 = H_1\delta^2$, $\sigma^2_{\delta,\mathrm{CSR}} = \langle\delta^2\rangle$, ϵ is the unperturbed geometric emittance, and γ is the relativistic Lorentz factor. From the physical point of view, Eq. (6) describes the chromatic, but reversible dilution of the emittance in a dispersive element. The initial energy kick is transmitted to the transverse plane via the H function, and the effect is later on modulated via α at the dipole locations. For completeness, the same approach as in Eqs. (1)–(4) was applied to a dog-leg-like achromatic line with only two dipoles. In this case the phase advance that fully cancels the CSR kicks is $2n\pi$, and the final particle invariant is

$$2J_f = 2J_i\left[\left(1 - \sqrt{\frac{\beta_i}{\beta_f}}\right)^2 + \left(\alpha_i\sqrt{\frac{\beta_f}{\beta_i}} + \alpha_f\sqrt{\frac{\beta_i}{\beta_f}}\right)^2\right], \quad (7)$$

where the subscripts f and i refer to the first and the second dipoles, respectively. The adoption of an odd or even multiple of the π phase advance between the dipoles changes the sign in the first squared term of Eq. (7). The sign of the curvature of one of the dipoles affects the signs of both the squared terms. Therefore, the idea reported in Ref. [1] (π phase advance between two identical dispersive elements) is a special case of the present treatment that, in agreement with [1], requires a fully symmetric optics for the complete CSR suppression.

The parameters of the electron beam and of the line that characterize our experiment are listed in Table I. The bunch length was magnetically compressed at 300 MeV by a factor CF = 8 in a first experimental session and by CF = 16 in a second one. The beam optics was matched [30] to the Spreader nominal lattice (see Fig. 2) with a mismatch parameter [31] $\xi \cong 1.05$ in both transverse planes. The rms projected emittance was measured with the quadrupole scan technique [32] at the beginning and at the end of the Spreader, in regions nominally free of momentum dispersion. Details about the emittance measurement can be found in Ref. [19]. Standard error propagation led to typical errors of a few percent on the central value of the beam optical parameters. A nonzero spurious dispersion was measured in the proximity of the screen used for the final emittance measurement. The dispersion value was the resultant of a linear, least means-square fit applied to the beam position measured as the beam mean energy was varied over a normalized range of $\pm 1.0\%$ [33]. The dispersion uncertainty was dominated by the measurement reproducibility. The emittance and the dispersion were scanned versus the strength of a quadrupole (Q_SFEL01.02) placed between the two MDBAs, as shown in Fig. 3. While the nominal quadrupole setting is expected to cancel the CSR kicks by implementing asymmetric but properly balanced optics in the two MDBAs with $\Delta\mu = \pi$ between the two achromats, any deviation from this setting would affect both the phase advance and the C-S parameters in the second MDBA, thus breaking the optics balance. The phase advance was computed with the ELEGANT code [34] on the basis of the real machine setting, and it is

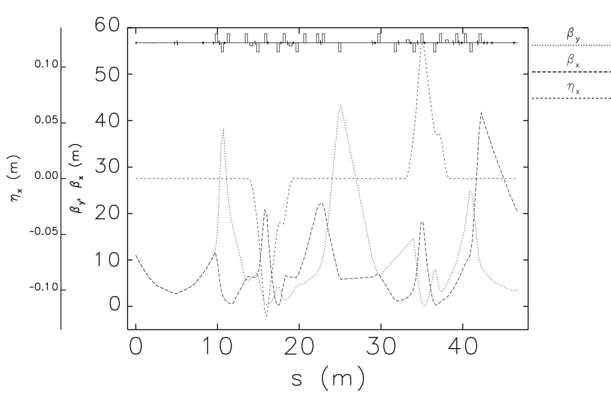

FIG. 2. Nominal optics of the Spreader. The two MDBAs are identified by the closed dispersion bumps. The machine layout is sketched at the top.

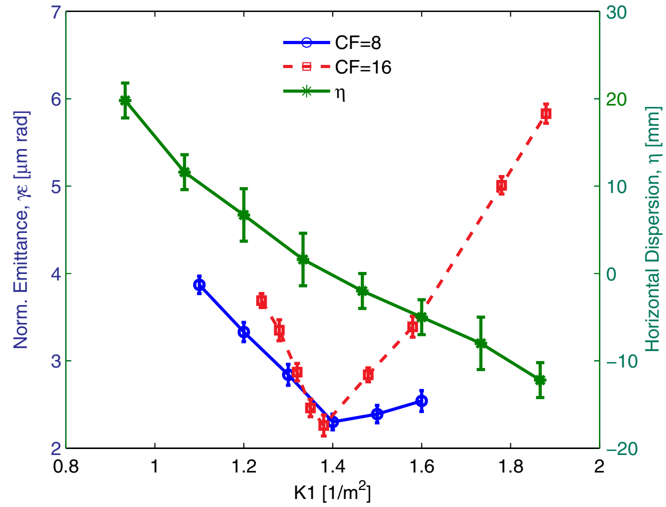

FIG. 3 (color online). Horizontal emittance (circles for CF = 8, squares for CF = 16) and spurious horizontal dispersion (stars) measured at the Spreader end versus the strength of the quadrupole Q_SFEL01.02 placed between the two MDBAs.

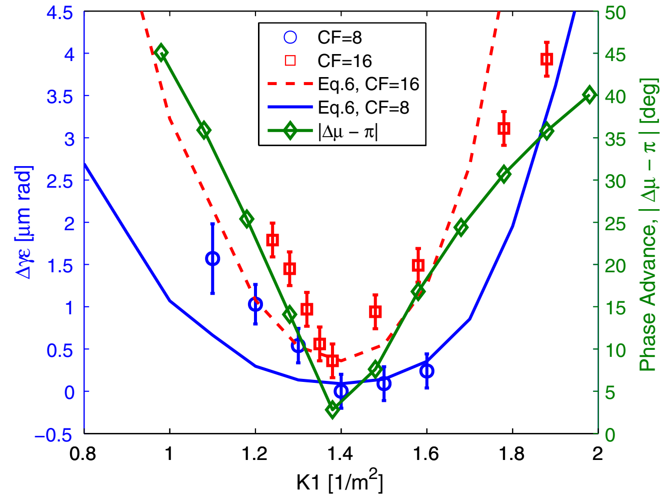

FIG. 4 (color online). The horizontal normalized emittance growth at the end of the Spreader (markers with error bars) is plotted as a function of the strength of the quadrupole Q_SFEL01.02 placed between the two MDBAs. The squares (circles) are for a compression factor of 16 (8). The horizontal betatron phase advance between the MDBAs (diamonds) was computed with ELEGANT on the basis of the experimental machine settings; the absolute value of its distance from π is also shown. The dashed (solid) line is the evaluation of Eq. (6) for CF = 16(8).

plotted in Fig. 4 together with the final emittance increment as the strength of Q_SFEL01.02 was varied. As predicted, almost zero emitttance growth was observed when the phase advance between the MBDAs was π. As we vary the quadrupole strength away from its optimal setting, the emittance grows with a higher rate for the shorter beam. This can be explained by the fact that the CSR induced energy spread and the associated CSR kicks are inversely proportional to the bunch length [15]. Finally, Eq. (6) was evaluated on account that the analysis is expected to fit well the experiment when the phase advance is close to π (this is an assumption of our mathematical model) and to diverge for larger distances from that value. This behavior is experimentally confirmed in Fig. 4, where the minimum emittance growth (π phase advance) matches well the theoretical value. The error bars in Fig. 4 are computed as the square-root sum of the errors of the initial and final emittances (reported in Table I and Fig. 3, respectively) and the contribution from the spurious dispersion, namely $\Delta\gamma\varepsilon_\eta \approx \frac{\gamma(\eta\sigma_\delta)^2}{\beta}$. In this case, the total relative energy spread is the square-root sum of the initial energy spread ($\sigma_\delta \sim 10^{-3}$; see Table I) and of that induced by the CSR emission ($\approx 4 \times 10^{-4}$ and $\approx 2 \times 10^{-4}$ for CF = 16 and CF = 8, respectively). Given our beam parameters and the dipoles' geometry, the latter was computed in the so-called long bunch, long magnet regime of CSR emission [15,19] and used for the evaluation of Eq. (6). Although a discrepancy at phase advances far from π is expected, other effects might be contributing to it. For instance, by varying the quadrupole strength in between the two MDBAs we were exciting some spurious dispersion that might have been corrupting the symmetry assumed for η and η' at all the dipoles, thus affecting the efficiency of CSR cancellation.

In conclusion, the original idea for the suppression of CSR kicks with optics symmetry [1] is explained in this Letter by applying the C-S formalism to dog-leg-like achromatic lines. Alternative solutions with asymmetric optics are allowed, as shown by Eq. (5). More precisely, this analytical result allows for the evaluation of the final emittance growth as a function of the optics asymmetry, and thus it applies also to asymmetric designs that may be required by other than optical constraints. Asymmetric, but properly balanced optics were present in the FERMI Spreader, together with the relative phase advance of π between the achromats, allowing for the preservation of the 2 μm normalized emittance of 500 pC, 40 μm, and 80 μm long bunches. The emittance growth was measured as the phase advance was changed and the optics balance was broken. The growth rate was higher for the shorter beam, in agreement with the expected CSR dynamics, and the experimental behavior is well described by the analytical model. The results presented in this Letter suggest that compact dispersive lines can be designed and built in future high brightness electron accelerators, such as linac-based FELs or linear colliders. This study should be continued and extended in order to further explore the development of the CSR instability in the presence of larger bending angles ($\geq 10°$) and very short beams (~ 1 μm). A detailed simulation study that would include the propagation of CSR in the drift sections is pending.

W. Fawley is acknowledged for stimulating discussions about the optics design and matching in the FERMI

Spreader. G. Penco and M. Trovo' are the authors of the codes used for the emittance measurement. L. Froehlich is the author of the code for the dispersion measurement.

---

[1] D. Douglas, Thomas Jefferson National Accelerator Facility Report No. JLAB-TN-98-012, 1998.

[2] E. D. Courant and H. S. Snyder, Ann. Phys. (N.Y.) **3**, 1 (1958); See also S. Y. Lee, *Accelerator Physics* (World Scientific, Singapore, 2007), ISBN.

[3] C. Bocchetta *et al.*, FERMI@Elettra Report No. ST/F-TN-07/12, 2007, http://www.elettra.trieste.it/FERMI/index.php?n=Main.CDRdocument.

[4] P. Emma *et al.*, Nat. Photonics **4**, 641 (2010).

[5] W. Ackermann *et al.*, Nat. Photonics **1**, 336 (2007).

[6] D. Pile, Nat. Photonics **5**, 456 (2011).

[7] M. Altarelli, Nucl. Instrum. Methods Phys. Res., Sect. B **269**, 2845 (2011).

[8] International Linear Collider, Reference Design Report, 2007, http://www.linearcollider.org/about/Publications/Reference-Design-Report.

[9] J. Ellis and I. Wilson, Nature (London) **409**, 431 (2001).

[10] R. Talman, Phys. Rev. Lett. **56**, 1429 (1986).

[11] T. Nakazato, M. Oyamada, N. Niimura, S. Urasawa, O. Konno, A. Kagaya, R. Kato, T. Kamiyama, Y. Torizuka, T. Nanba, Y. Kondo, Y. Shibata, K. Ishi, T. Ohsaka, and M. Ikezawa, Phys. Rev. Lett. **63**, 2433 (1989).

[12] Ya. S. Derbenev, J. Rossbach, E. L. Saldin, and V. D. Shiltsev, Deutsches Elektronen-Synchrotron Report No. TESLA-FEL 95-05, 1995.

[13] B. E. Carlsten and T. O. Raubenheimer, Phys. Rev. E **51**, 1453 (1995).

[14] Ya. S. Derbenev and V. D. Shiltsev, Stanford Linear Accelerator Center Report No. SLAC-PUB-7181, 1996.

[15] E. L. Saldin, E. A. Schneidmiller, and M. V. Yurkov, Nucl. Instrum. Methods Phys. Res., Sect. A **398**, 373 (1997).

[16] R. Li and Ya. S. Derbenev, Thomas Jefferson National Accelerator Facility Report No. JLAB-TN-02-054, 2002.

[17] M. Dohlus and T. Limberg, Nucl. Instrum. Methods Phys. Res., Sect. A **393**, 494 (1997).

[18] H. Braun, F. Chautard, R. Corsini, T. O. Raubenheimer, and P. Tenenbaum, Phys. Rev. Lett. **84**, 658 (2000).

[19] S. Di Mitri, E. M. Allaria, P. Craievich, W. Fawley, L. Giannessi, A. Lutman, G. Penco, S. Spampinati, and M. Trovo, Phys. Rev. ST Accel. Beams **15**, 020701 (2012).

[20] P. Emma and R. Brinkmann, Stanford Linear Accelerator Center Report No. SLAC-PUB-7554, 1997.

[21] J. S. Nodvick and D. Saxon, Phys. Rev. **96**, 180 (1954).

[22] R. L. Warnock, Stanford Linear Accelerator Center Report No. SLAC-PUB-5375, 1990.

[23] G. V. Stupakov and I. A. Kotelnikov, Phys. Rev. ST Accel. Beams **6**, 034401 (2003).

[24] E. L. Saldin, E. A. Schneidmiller, and M. V. Yurkov, Nucl. Instrum. Methods Phys. Res., Sect. A **490**, 1 (2002).

[25] S. Heifets, S. Krinsky, and G. Stupakov, Phys. Rev. ST Accel. Beams **5**, 064401 (2002).

[26] Z. Huang and K.-J. Kim, Phys. Rev. ST Accel. Beams **5**, 074401 (2002).

[27] Z. Huang, M. Borland, P. Emma, J. Wu, C. Limborg, G. Stupakov, and J. Welch, Phys. Rev. ST Accel. Beams **7**, 074401 (2004).

[28] A. Zholents, K. Chow, R. Wells, D. Bacescu, B. Diviacco, M. Ferianis, and S. Di Mitri, Elettra-Sincrotrone Trieste Report No. ST/F-TN-07/01, 2007; Report No. LBNL-62345, 2007. The design lattice was later modified by one of the authors (S. Di Mitri).

[29] A. Jackson, Part. Accel. **22**, 111 (1987).

[30] S. Di Mitri, M. Cornacchia, C. Scafuri, and M. Sjostrom, Phys. Rev. ST Accel. Beams **15**, 012802 (2012).

[31] M. Sands, Stanford Linear Accelerator Center Report No. SLAC-AP-85, 1991.

[32] M. G. Minty and F. Zimmermann, Stanford Linear Accelerator Center Report No. SLAC-R-621, 2003.

[33] S. Di Mitri, L. Froehlich, and E. Karantzoulis, Phys. Rev. ST Accel. Beams **15**, 061001 (2012).

[34] M. Borland, Advanced Photon Source Report No. LS-287, 2000.